Journal of Power Sources 196 (2011) 6742–6749

Contents lists available at ScienceDirect

Journal of Power Sources

journal homepage: www.elsevier.com/locate/jpowsour

Preparation and electrochemical characterization of gel polymer electrolyte based on electrospun polyacrylonitrile nonwoven membranes for lithium batteries

Prasanth Raghavan[a], James Manuel[a], Xiaohui Zhao[a], Dul-Sun Kim[a], Jou-Hyeon Ahn[a,*], Changwoon Nah[b]

[a] Department of Chemical and Biological Engineering and Engineering Research Institute, Gyeongsang National University, 900, Gajwa-dong, Jinju 660-701, Republic of Korea
[b] Department of Polymer-Nano Science and Technology, Chonbuk National University, 664-14, Duckjin-dong, Jeonju 561-756, Republic of Korea

ARTICLE INFO

Article history:
Received 16 August 2010
Received in revised form 25 October 2010
Accepted 26 October 2010
Available online 2 November 2010

Keywords:
Electrospinning
Fibrous membrane
Polymer separator
Gel polymer electrolyte
Polyacrylonitrile

ABSTRACT

Electrospun membranes of polyacrylonitrile are prepared, and the electrospinning parameters are optimized to get fibrous membranes with uniform bead-free morphology. The polymer solution of 16 wt.% in *N*,*N*-dimethylformamide at an applied voltage of 20 kV results in the nanofibrous membrane with average fiber diameter of 350 nm and narrow fiber diameter distribution. Gel polymer electrolytes are prepared by activating the nonwoven membranes with different liquid electrolytes. The nanometer level fiber diameter and fully interconnected pore structure of the host polymer membranes facilitate easy penetration of the liquid electrolyte. The gel polymer electrolytes show high electrolyte uptake (>390%) and high ionic conductivity (>2×10^{-3} S cm^{-1}). The cell fabricated with the gel polymer electrolytes shows good interfacial stability and oxidation stability >4.7 V. Prototype coin cells with gel polymer electrolytes based on a membrane activated with 1 M $LiPF_6$ in ethylene carbonate/dimethyl carbonate or propylene carbonate are evaluated for discharge capacity and cycle property in Li/$LiFePO_4$ cells at room temperature. The cells show remarkably good cycle performance with high initial discharge properties and low capacity fade under continuous cycling.

1. Introduction

Gel polymer electrolytes (GPEs) have received considerable attention in recent years for application in rechargeable secondary batteries, fuel cells, supercapacitors, etc., since they can offer systems that are lighter, safer and more flexible in shape compared with their liquid counterparts [1,2]. The host polymers reported for the preparation of GPEs include poly(vinylidene fluoride) (PVdF) [3–5] and its copolymer poly(vinylidene fluoride-*co*-hexafluoropropylene) {P(VdF-*co*-HFP)} [1,2,6–9], poly(ethylene glycol) (PEG) [10], poly(urethane acrylate) (PUA) [11], polyacrylonitrile (PAN) [12], poly(methyl methacrylate) (PMMA) [13] and poly(ethylene oxide) (PEO) [14]. In our previous studies we evaluated the electrochemical properties of GPEs based on electrospun P(VdF-*co*-HFP). The GPEs showed good electrochemical stability, high affinity to electrolyte solutions, and desirable adhesion with the electrode, and exhibited ionic conductivities in the range of 10^{-4} to 10^{-3} S cm^{-1} at room temperature [1,2,6–9]. P(VdF-*co*-HFP) has high dielectric constant and electron withdrawing fluorine atoms in the polymer backbone structure. These features are advantageous to dissociate the lithium salt to lithium ions while transforming into polymer electrolyte. The formation of stable LiF and >C=CF– unsaturated bonds through interactions between the fluorine atoms in PVdF part of the polymer and lithium or lithiated graphite is one of the problems to restrict the use of P(VdF-*co*-HFP) based membranes for polymer electrolyte, which not only deteriorate the battery performance but also raise safety concerns, because of thermal runway caused by the highly exothermic reactions [15]. It has been reported that PVdF-based membranes are miscible with liquid electrolytes that are generally used for the preparation of GPEs [16,17]. Therefore, a multiphase electrolyte consisting of liquid electrolyte and gel polymer electrolyte is often formed when PVdF-based membrane is used as separator in lithium ion batteries. This could result in loss of mechanical strength and internal short-circuits. The crystalline part of P(VdF-*co*-HFP) hinders the migration of Li^+ ions and hence batteries with P(VdF-*co*-HFP) based electrolytes have lower charge/discharge capacities and poor C-rate values [18].

Aiming to resolve these problems, we found that PAN is a good substitute for the PVdF or its copolymers [19]. PAN has good processability, flame resistance, resistance to oxidative degradation and electrochemical stability. Oxidative stabilization of PAN is very

* Corresponding author. Tel.: +82 55 751 5388; fax: +82 55 753 1806.
E-mail address: jhahn@gnu.ac.kr (J.-H. Ahn).

0378-7753/$ – see front matter © 2010 Elsevier B.V. All rights reserved.
doi:10.1016/j.jpowsour.2010.10.089

high even at high temperature. PAN-based polymer electrolyte has shown interesting characteristics like high ionic conductivity, thermal stability, good morphology for electrolyte uptake and compatibility with lithium electrode. Tsutsumi et al. reported that PAN-based gel polymer electrolytes minimize the formation of dendrite growth during the charging/discharging processes of lithium batteries [20]. PAN based GPE was prepared by a phase inversion method and the electrolyte behavior was reported [21,22].

The porous PAN membranes are very brittle for the reason that the interaction of adjacent cyanide groups increases the resistance of interior rotation of the main chain and thus decreases the flexibility of the main chain [23]. Electrospinning is an alternative, efficient and simple method to prepare thin fibrous porous membranes with high level of porosity [1]. PAN contains highly polar nitrile groups, hindering the alignment of macromolecular chains during electrospinning and hence it can be made as a flexible membrane with good mechanical strength. This study involves the optimization of process parameters for preparing nanofibrous PAN membranes with uniform morphology. The GPEs based on the fibrous membranes were prepared by the activation of the membranes with different liquid electrolytes, and their electrochemical properties were evaluated.

2. Experimental

2.1. Preparation and characterization of electrospun membranes

PAN (MW 150,000, Polysciences) was vacuum dried at 60 °C for 6 h before use. The solvent *N*,*N*-dimethylformamide (DMF) (Aldrich) was used as received. Fibrous membranes were prepared by the typical electrospinning method at room temperature, as described in our previous publications [1,2]. Homogeneous solution of PAN with various concentrations (10–18 wt.%) was prepared in DMF by mechanical stirring using high energy ball mill for 1 h at room temperature. The resulting solution was degassed for 15 min to get the clear solution. The polymer solution was supplied to a steel needle of bore size 0.6 mm through a capillary using a syringe infusion/withdrawal pump (KD Scientific, Model 210). High electric voltage (varied 10–25 kV) was applied to polymer solution by clamping the electrode of the power supply at the tip of the steel needle. A grounded, stainless-steel current collector in the shape of a drum covered with a thin aluminum foil, rotating at specified speed was used as the target for collecting PAN fibers in the form of nonwoven membrane. The essential electrospinning parameters were as follows: applied voltage 10–25 kV, distance between the tip of the spinneret and collector 20 cm, needle size 0.6 mm, solution feed rate 0.1 mL min^{-1} and collector drum rotation speed 140 rpm. Electrospun membranes of average thickness 100 μm were collected and dried at room temperature on the drum for 6 h to prevent the shrinking of fibers and then vacuum dried at 60 °C for 12 h before further use.

The surface morphology of the fibrous membranes was investigated with a high resolution field emission scanning electron microscope (FE-SEM-JEOL JSM 5600). The average fiber diameter (AFD) was determined from the micrographs taken at high magnifications and about 250 fibers were investigated. The porosity (*P*) was determined by *n*-butanol uptake method [1].

2.2. Preparation of GPEs based on electrospun fibrous membranes

Electrospun PAN based GPEs were prepared by soaking the circular membrane of about 2 cm^2 area for 1 h in lithium salt-based liquid electrolytes, such as 1 M lithium hexafluorophosphate ($LiPF_6$) in (i) ethylene carbonate (EC)/dimethyl carbonate (DMC) (1:1, v/v); (ii) EC/diethyl carbonate (DEC) (1:1, v/v); (iii) EC/ethyl methyl carbonate (EMC) (1:1, v/v), and (iv) propylene carbonate (PC) under argon atmosphere in a glove box (H_2O < 10 ppm) at room temperature. The lithium salts and organic solvents were supplied by Aldrich.

2.3. Electrochemical measurements

The fibrous membrane prepared with solution concentration of 16 wt.% and applied voltage of 20 kV was used for further electrochemical studies. Electrolyte uptake by the membrane was determined by soaking a circular piece of the membrane (diameter 1.6 cm) in each electrolyte solution as reported elsewhere [1]. The weight of the wetted membrane was determined at different soaking intervals, taking care to remove the excess electrolyte remaining on the surface of the membrane by wiping softly with a tissue paper. The ionic conductivity of the GPEs, over the temperature range −20 to 80 °C, was measured by the AC impedance analysis using stainless-steel (SS) Swagelok® cells with an IM6 frequency analyzer. The measurements were performed over the frequency range of 100 mHz to 2 MHz at an amplitude of 20 mV. The electrochemical stability was determined by linear sweep voltammetry (LSV) of Li/GPE/SS cells at a scan rate of 1 mV s^{-1} over the range of 2–6 V at 25 °C. The time dependent interfacial resistance (R_f) between the GPE and lithium metal electrode was measured by the impedance response of Li/GPE/Li cells over the frequency range 100 mHz to 2 MHz at an amplitude of 20 mV. The prototype lithium cell of 23 mm diameter was fabricated by sandwiching the fibrous membrane based GPE between a lithium metal anode (300 μm thickness, Cyprus Foote Mineral Co.) and lithium iron phosphate ($LiFePO_4$) cathode. The carbon-coated $LiFePO_4$ cathode active material was made in-house by mechanical activation followed by solid-state reaction at high temperature [24]. The charge–discharge and cycling tests were conducted in an automatic galvanostatic charge–discharge unit, WBCS3000 battery cycler (WonA Tech. Co.), between 2.5 and 4.0 V at room temperature. The experiments were run at a current density rate of 0.1 C.

3. Results and discussion

3.1. Optimization of electrospinning parameters and membrane characterization

There are lots of parameters governing the fiber diameter and morphology of the electrospun membranes. These parameters include solution properties such as viscosity, conductivity, surface tension; governing variables like hydrostatic pressure in capillary, electric potential at capillary tip, gap between capillary tip and collecting drum; ambient parameters like solution temperature, humidity and air velocity in the electrospinning chamber [25]. In our previous studies we optimized the process parameters to obtain membranes that consist of bead-free fibers with uniform size and well defined morphology with P(VdF-*co*-HFP) [4]. In the present study we follow the same parameters with varying solution concentration and applied voltage to study the effect of the variables on the morphology of the PAN based membranes.

SEM images along with fiber diameter distribution of the membranes prepared at different solution concentrations and applied voltages are given in Figs. 1 and 2. The micrographs show a three dimensional network structure with fully interconnected pores made up of ultrafine fibers. This indicates that dry fibers are deposited by rapid evaporation of the solvent during electrospinning. The variation of processing conditions along with fiber diameter range and AFD of the membranes obtained under the studied conditions are presented in Table 1. SEM images of Figs. 1 and 2(c) show the effect of change in concentration of the

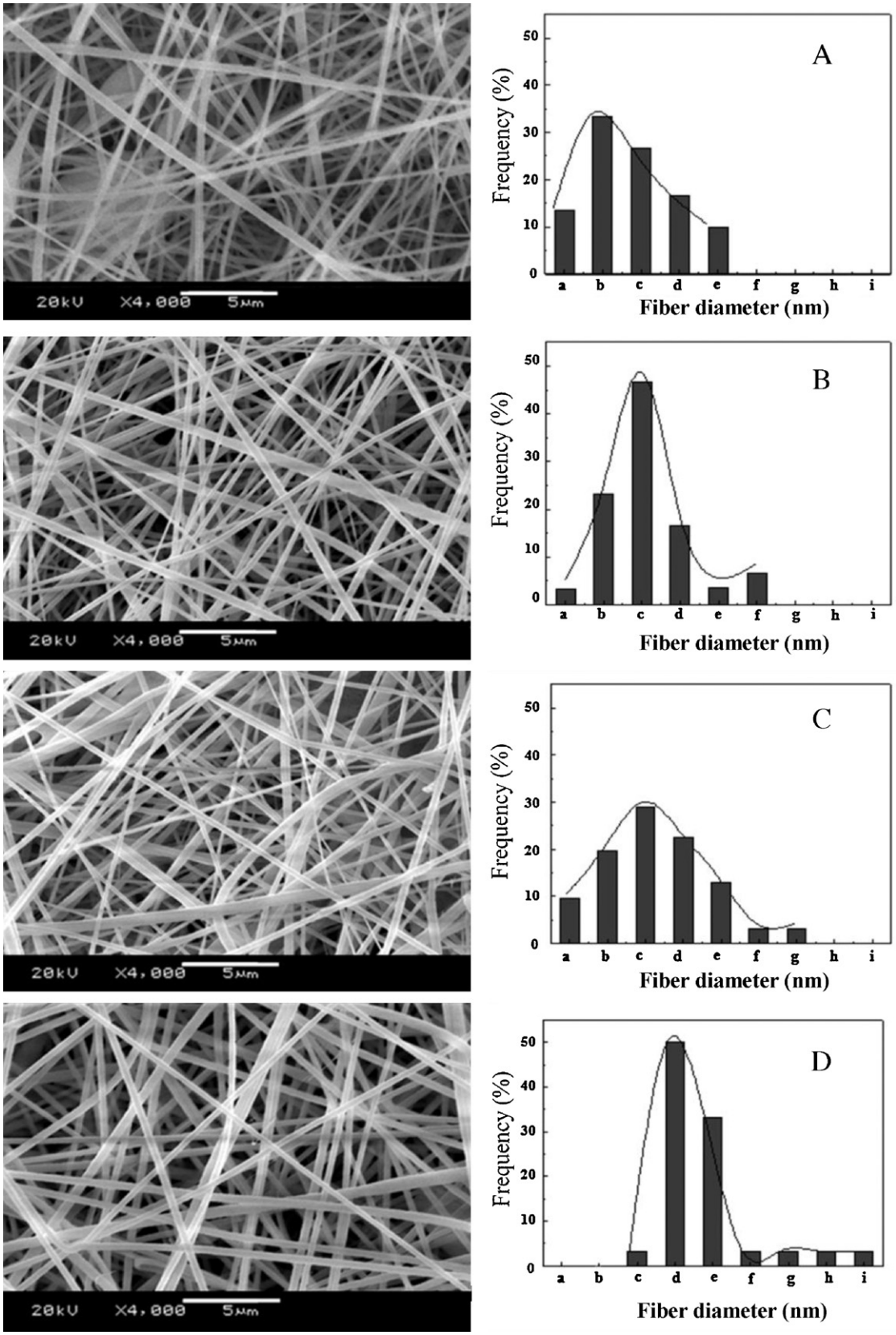

Fig. 1. SEM images and fiber diameter distribution of electrospun polyacrylonitrile fibrous membranes prepared with different polymer concentrations (wt.%): (A) 10, (B) 12, (C) 14 and (D) 18; applied voltage: 20 kV; fiber diameter range (nm); (a) 80–150, (b) 151–230, (c) 231–330, (d) 331–410, (e) 411–490, (f) 491–580, (g) 581–660, (h) 661–740, (i) 741–820.

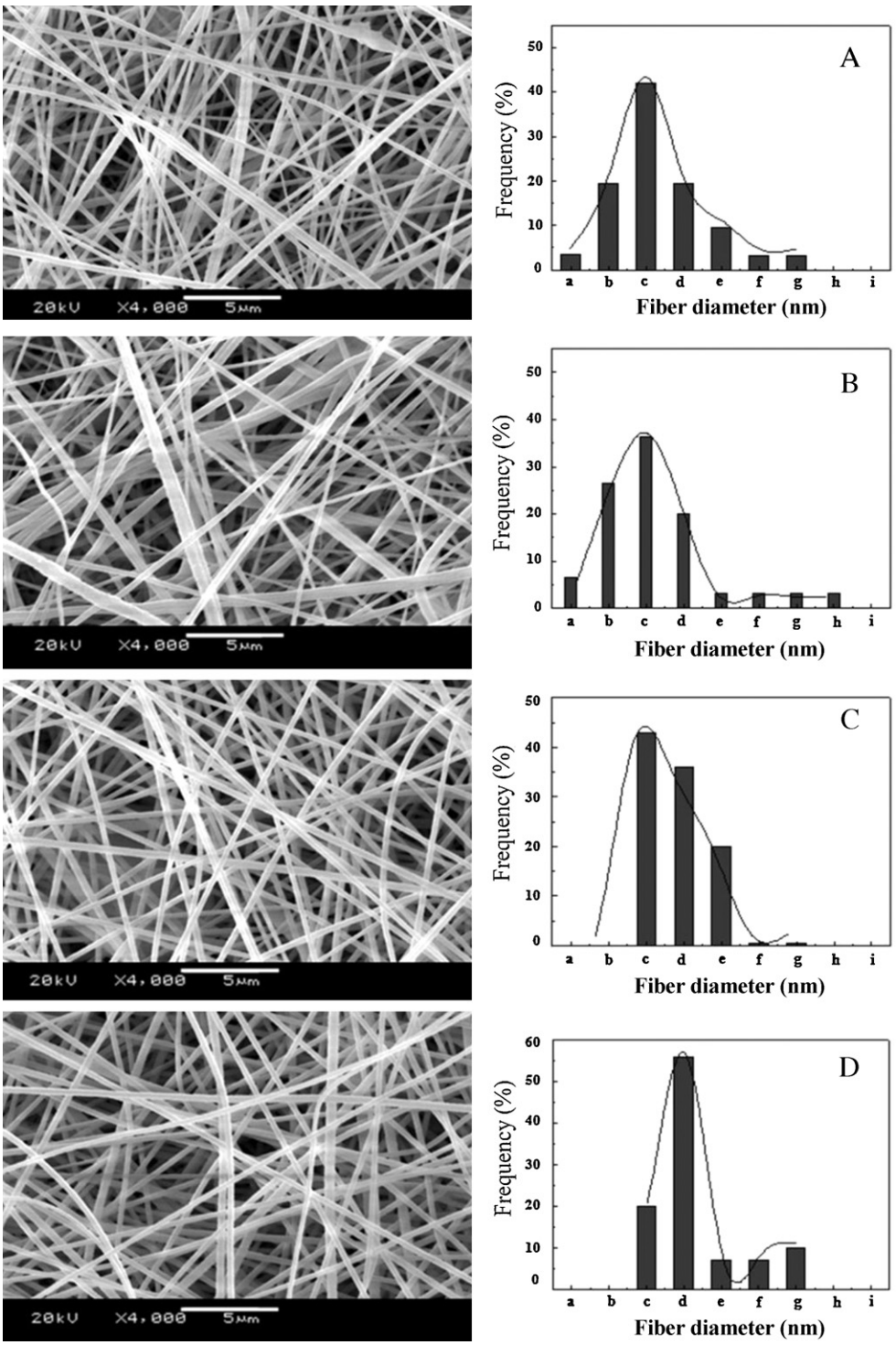

Fig. 2. SEM images and fiber diameter distribution of electrospun polyacrylonitrile fibrous membranes prepared with different applied voltages (kV): (A) 10, (B) 15, (C) 20 and (D) 25; polymer concentration: 16 wt.%; fiber diameter range (nm): (a) 80–150, (b) 151–230, (c) 231–330, (d) 331–410, (e) 411–490, (f) 491–580, (g) 581–660, (h) 661–740, (i) 741–820.

polymer solution from 10 to 18 wt.% on the morphology and AFD of the membranes at an applied voltage of 20 kV. It is found that the polymer concentration has a marked influence on the AFD and morphology of the membranes. The AFD of the membranes increases with increasing polymer concentration. This results from the higher viscosity of the polymer solution which is directly proportional to the solution concentration. Higher solution viscosity leads to the ejection of larger drops of the solution from the needle which forms larger fibers on the collection drum [26]. At lower concentration (10, 12 and 14 wt.%), the fiber diameter range is broad and the morphology is not uniform. With 10 wt.% solution the membrane showed poor morphology partially with a bead form and a wide range of fiber diameter distribution. This shows that the concentration of 10 wt.% solution might be the critical solution concentration to obtain good nanofibers with narrow fiber diameter distribution for electrospinning of PAN. Uniform membrane morphology with

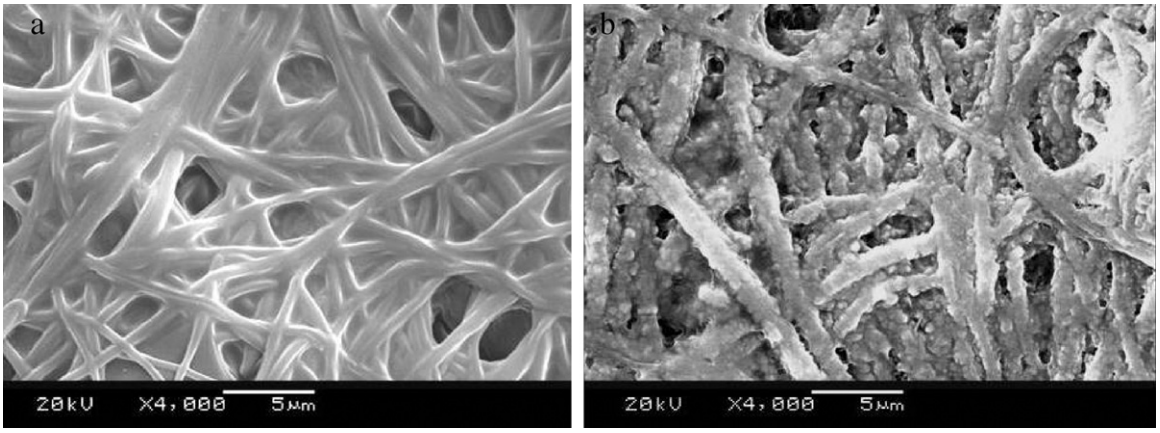

Fig. 3. SEM images of electrospun polyacrylonitrile fibrous membrane soaked in 1 M $LiPF_6$ in EC/DMC (1:1 v/v) (a) after 1 h, (b) after 750 h. The membrane was prepared with a polymer concentration of 16 wt.% and an applied voltage of 20 kV.

very narrow range of fiber diameter and an AFD of 350 nm was obtained by electrospinning of 16 wt.% solution at 20 kV. The optimized solution concentration was selected as 16 wt.% to study the effect of applied voltage on the morphology and fiber diameter of the membrane.

SEM images (Fig. 2) show the effect of applied voltage ranging from 10 to 25 kV on the morphology and fiber diameter of the membranes. It is found that the applied voltage also has considerable effect on the morphology of the membrane. In general higher applied voltage ejects more fluid in the jet and thereby leads to the formation of fibers with larger fiber diameter [26]. The same trend is also shown in this study. An applied voltage of 20 kV is found to be the optimum for obtaining the most uniform fiber morphology with straight fibers having narrow distribution of fiber diameter. Application of higher voltage results in the formation of considerable amount of large fibers with narrow range of fiber diameter. At lower voltage the AFD of the fibers was lower, but it shows wide range of fiber diameter. Also the fibers are not completely bead free and as straight as those with 20 kV.

The interlaying of fibers generates porous structure in the electrospun membrane. The porosity of the membrane varies in a narrow range of 84–86% showing a slight increase with increasing the solution concentration and the maximum value at 16 wt.%. Applied voltage also has a little influence on the porosity of the membrane, showing that as the applied voltage increases the porosity slightly increases. The difference in porosity is attributed to the three dimensional packing structure of the membrane depending on the polymer concentration and applied voltage. It is considered that the more porous network in the latter resulted from the loose packing of fibers in the layers of the membranes due to the combined effect of both applied voltage and polymer concentration. The high porosity of the membranes was also reflected in their high electrolyte uptake of electrolyte solution with 395, 415, 434, 479 and 455% obtained for the membranes prepared with polymer concentrations of 10, 12, 14, 16 and 18%, respectively, at the same applied voltage of 20 kV. The absorption of the large quantities of liquid electrolyte by the membrane results from the high porosity of the membrane and the partial gelation of the PAN membrane. The gelation of PAN membrane is attributed to its affinity for electrolyte solution, which results from the polar functional groups in PAN [22]. SEM images (Fig. 3) of the membrane after soaking in the electrolyte are evident for the same.

The fully interconnected pore structure facilitates fast penetration of the liquid electrolyte into the membrane, and hence the uptake process was stabilized within a time span of 15 min. Fig. 4 shows the comparison of electrolyte uptake, 1 M $LiPF_6$ in EC/DMC, of the membranes prepared with different polymer concentration at an applied voltage of 20 kV. The difference in electrolyte uptake is attributed to the difference in morphology, packing of fibers and its AFD, porosity and pore structure. The electrolyte uptake of the fibrous membrane in the present study is comparatively higher, showing a direct consequence of the higher porosity and fully interconnected pore structure achieved. Nevertheless, the membrane has good wettability by the electrolyte and a higher electrolyte uptake compared with that reported for the Celgard polyolefin separator (uptake ~130%, porosity ~40%) [27]. It is found that the uptake process is very fast for all electrolytes as shown in Fig. 4, and the maximum amount of liquid penetrates into the membrane within the initial few minutes. The high polarity of PAN [28] and fully interconnected pore structure of the membrane are beneficial in achieving this. The electrospun membrane exhibits sufficient mechanical strength and self-standing properties even after being activated with the liquid electrolytes. Commercially available polyolefin separators do not readily absorb the electrolyte solvents with high dielectric constants, such as EC, PC, and DMC because of their hydrophobic surface with low surface

Table 1
Morphological characteristics of electrospun polyacrylonitrile fibrous membranes under different processing parameters.

Polymer concentration (wt.%)	Applied voltage (kV)	FDR (μm)[a]	AFD (μm)[b]	Porosity (%)	Maximum uptake (%)
10	20	0.08–0.49	0.28	80	395
12	20	0.08–0.58	0.30	82	415
14	20	0.08–0.66	0.32	83	434
18	20	0.24–0.82	0.44	84	455
16	10	0.08–0.66	0.32	83	405
16	15	0.08–0.74	0.33	84	448
16	20	0.24–0.66	0.35	86	479
16	25	0.24–0.66	0.40	86	474

[a] Fiber diameter range.
[b] Average fiber diameter.

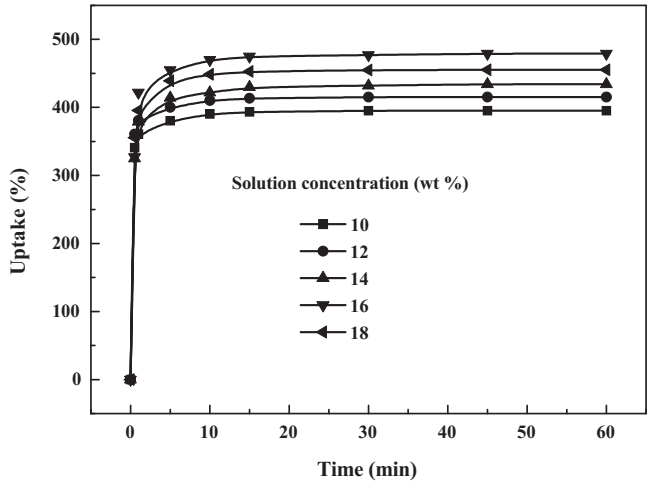

Fig. 4. Electrolyte uptake (%) of electrospun polyacrylonitrile fibrous membranes prepared with different polymer concentrations (wt.%); applied voltage: 20 kV; electrolyte: 1 M $LiPF_6$ in EC/DMC (1:1 v/v).

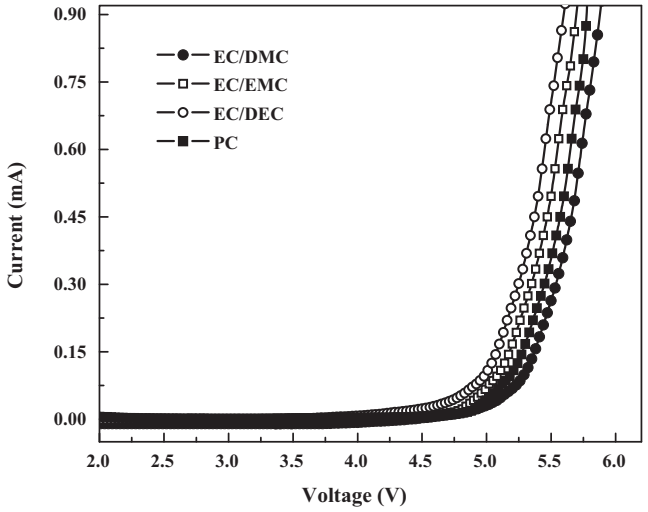

Fig. 6. Electrochemical stability by linear sweep voltammetry of gel polymer electrolytes based on electrospun polyacrylonitrile fibrous membrane with different liquid electrolytes (Li/GPE/SS cells, 1 mV s^{-1}, 2–6 V).

energy, and they have poor ability to retain the electrolyte solutions [29,30].

3.2. Ionic conductivity

The ionic conductivity of the GPEs was measured at different temperatures by the AC impedance method. The GPEs under the study comprise a solid polymer fiber phase, a partially swollen amorphous fiber phase and a liquid electrolyte phase encapsulated in the pores of the membrane [27,31]. Two ion conduction paths have been postulated for porous-membrane based GPEs: one is high conduction path through the liquid electrolyte phase and the other is slow conduction path through the swollen polymer phase [31,32]. Fig. 5 shows the Arrhenius plot of ionic conductivity of the GPEs with different liquid electrolytes in the temperature range of −20 to 80 °C. The conductivity was sharply decreased below 0 °C, due to the freezing property of carbonate solvents in the electrolyte solutions. The GPE with 1 M $LiPF_6$ in EC/DEC (1:1 v/v) showed the highest ionic conductivity, whereas that with 1 M $LiPF_6$ in PC showed the lowest ionic conductivity. The ionic conductivity is increased in the order of PC < EC/DMC < EC/EMC < EC/DEC. This is because the linear carbonate solvent retards the freezing of the EC fraction in the electrolyte and high dielectric constant of the constituent EC in the solvent mixture, which is helpful by causing a high dissociation of the lithium salt. However, the electrolyte 1 M $LiPF_6$ in PC shows the lowest conductivity, and it is attributed to the high viscosity of the electrolyte (Table 2), which is 1.3–4.2 times greater than other solvents used. The higher viscosity of PC limits the mobility of ions in the electrolyte. Nevertheless, this GPE has a conductivity of 2.14×10^{-3} S cm^{-1} at 25 °C, which is sufficient for the practical applications in lithium batteries. The ionic conductivities of the electrospun PAN based GPEs were lower than that of the liquid electrolytes. This is due to the slow ion conduction path in the swollen PAN fiber phase and the tortuosity of the pore structure.

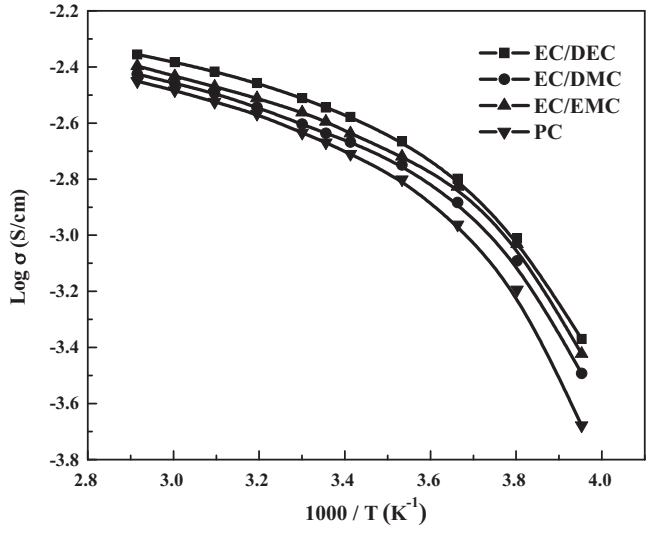

Fig. 5. Variation of ionic conductivities with temperature of gel polymer electrolytes based on electrospun polyacrylonitrile fibrous membrane with different liquid electrolytes (SS/GPE/SS cells, 100 mHz to 2 MHz, 20 mV).

3.3. Electrochemical properties

The electrochemical stability of the GPEs by LSV is presented in Fig. 6. Although the ionic conduction occurs mainly through the entrapped liquid electrolyte in the porous structure, the partially swollen fibrous matrix with large surface area contributes significantly in enhancing the electrochemical stability of the GPE. All the PEs based on PAN studied here exhibit an anodic stability greater than 4.7 V versus Li/Li^+. The high anodic stability results from the excellent affinity to the carbonate based liquid electrolyte solution which can partially swell the fibers. The swollen phase of the membrane includes the complex compounds such as associated $–CN–Li^+$ groups, the associated $–CO–Li^+$ groups and the associated $–CN–Li^+–OC$ groups. This complex formation with lithium ion and dipole–dipole interaction between the CO group of the carbonate molecules and the pendent CN group of the PAN greatly enhances the electrochemical stability of the resulting polymer electrolytes. The order of electrochemical stability (V) is 1 M $LiPF_6$ in EC/DMC (5.0) > PC (4.9) > EC/EMC (4.8) > EC/DEC (4.7). The earlier studies have also been reported high electrochemical stability for PEs based on electrospun PAN [33], PVdF [28,34] and P(VdF-*co*-HFP) [1–3,32]. The high anodic stability of these polymer electrolytes should render them potentially compatible with the high voltage cathode materials like $LiCoO_2$ and $LiMn_2O_4$ used commonly in lithium ion batteries.

Compatibility of the electrolyte with lithium metal anode is an important factor that determines the cycle performance of lithium

Table 2
Physical properties of carbonate based solvents in electrolytes.

Solvent	EC	DMC	EMC	DEC	PC
Molecular weight	88	90	104	118	102
Structure	Cyclic	Linear	Linear	Linear	Cyclic
Melting point (°C)	36.4	4.6	−53	−43.3	−48.8
Viscosity (cP at 25 °C)	1.93[40]	0.59[20]	0.65	0.73	2.53
Dielectric constant (25 °C)	89.78	3.11	2.96	2.81	64.92
Density at 25 °C (g cm^{-3})	1.321	1.063	1.000	0.969	1.200
Boiling point (°C)	243.5	90.3	109.0	126.8	240.0

cells. The impedance spectra of the GPEs in the form of semi circles typical of electrolytes with contribution from bulk electrolyte resistance (R_b) and electrode/electrolyte interfacial resistance (R_f) were observed. The real axis intercept at the high frequency end of the spectrum denote the R_b of the electrolyte and is very law (2–7 Ω). These values agree well with the low R_b value observed for the electrolytes in SS/GPE/SS cells (2–5 Ω). There was no appreciable increase in R_b with storage time up to 8 days. This behavior is indicative of a good retention of the ionic conductivity of the GPE consisting of a swollen fibrous structure.

The variation of interfacial resistance with storage time is represented in Fig. 7. It is found that the interfacial resistance increases with storage time to reach a maximum and then starts to decrease. The initial increase in R_f with time is inevitable in lithium metal batteries as it indicates the formation and growth of the passivation layer on the metal surface by reaction with the electrolyte components, impeding the passage of ions. The formation of passivation layer prevents further reaction of the electrolyte with lithium, helps to enhance the cathodic limit of the electrolyte, and thus improves cycling properties. It is found that R_f initially increased during 6 days, and decreased thereafter. The initial R_f values were 237, 290, 295, and 345 Ω, respectively for the PEs with EC/DEC, PC, EC/EMC, and EC/DMC. After 6 days, the R_f values increased from 124 to 196% as compared to the initial R_f values and then decreased. The initial increase in R_f may be due to the reaction of –CN group of PAN with lithium. However, it is found that the interfacial resistance is comparatively quite low and increases slowly upon storage time. These favorable interfacial properties reflect a good electrode behavior with GPE making it very promising candidate for safe, reliable and long lasting lithium batteries.

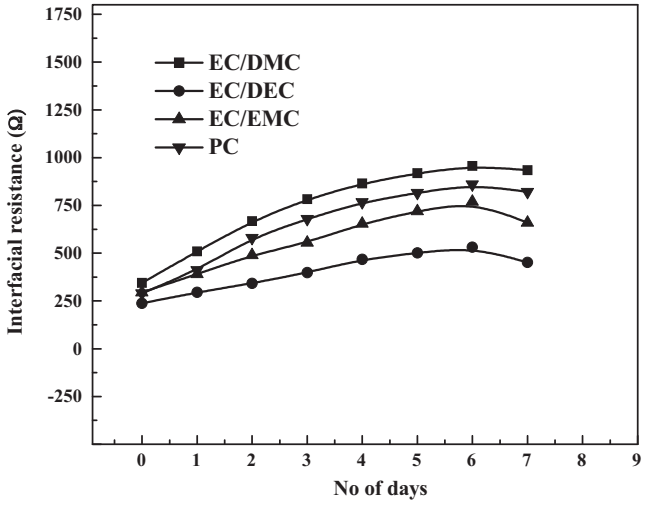

Fig. 7. Time dependent interfacial resistance of gel polymer electrolytes based on electrospun polyacrylonitrile fibrous membrane with different liquid electrolytes (Li/GPE/Li cells, 100 mHz to 2 MHz, 20 mV).

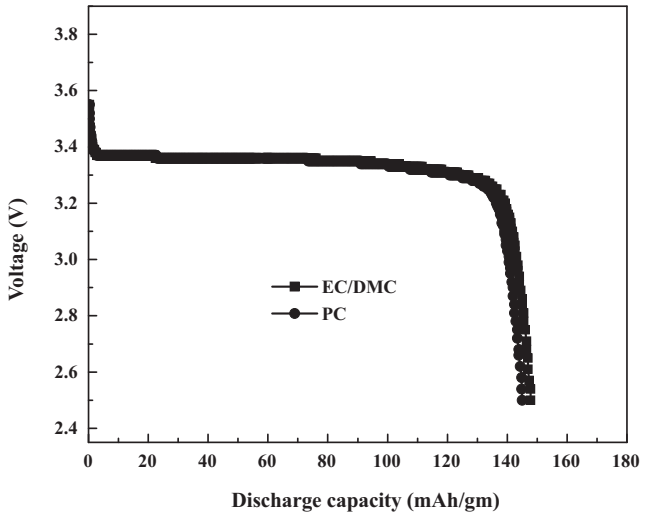

Fig. 8. Initial discharge properties of Li/LiFePO$_4$ cell using gel polymer electrolytes based on electrospun polyacrylonitrile fibrous membranes with different electrolytes; 1 M LiPF$_6$ in EC/DMC (1:1 v/v) and 1 M LiPF$_6$ in PC.

3.4. Evaluation in Li/LiFePO$_4$ cell

GPEs comprised of electrospun PAN with 1 M LiPF$_6$ in EC/DMC and PC was selected for the evaluation in a lithium metal battery with LiFePO$_4$ cathode at room temperature. LiFePO$_4$ has attracted much attention as the next generation cathode material. It has a high theoretical capacity of 170 mA h g^{-1}, an operating potential of

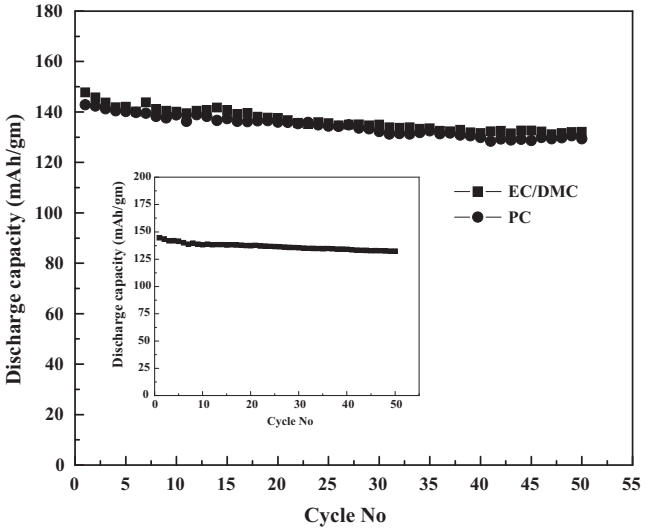

Fig. 9. Cycle performance of Li/LiFePO$_4$ cell using gel polymer electrolytes based on electrospun polyacrylonitrile fibrous membrane with different electrolytes; 1 M LiPF$_6$ in EC/DMC (1:1 v/v) and 1 M LiPF$_6$ in PC. Inset shows the cycle performance of Li/LiFePO4 cell assembled with 1 M LiPF6 in EC/DMC (1:1 v/v) using Celgard®-2200 separator under same conditions.

3.4 V, and excellent cycling properties. The initial discharge capacities at current density 0.1 C of Li/$LiFePO_4$ cell with electrospun PAN based GPEs are presented in Fig. 8. The cells show relatively high cathode utilization corresponding to discharge capacity of ~150 mA h g^{-1}, which is 88% of the theoretical capacity.

The cycle performance of the cells up to 50 cycles was studied as shown in Fig. 9. After 50 cycles, the cells retain 90% of initial discharge capacities which corresponds to 79% of the theoretical capacity. The discharge capacity fade of 0.24% per cycle was observed after 50th cycle (over initial capacity). The cycle performance of the cell with the liquid electrolyte of 1 M LiPF6 in EC/DMC using Celgard®-2200 separator is also shown in Fig. 9. It is seen that the performance of GPE based on electrospun PAN is as good as the liquid electrolyte. The capacity fade is also comparable for both the GPE and liquid electrolyte. The good cycle property of the cell can be attributed to enabling free passage of ions between electrodes, and good compatibility between the electrolyte and electrode, especially with lithium metal. This evaluation demonstrates the suitability of GPE based on electrospun PAN membrane for lithium battery applications.

4. Conclusions

Fibrous GPEs based on electrospun PAN were prepared by electrospinning of the polymer solution in DMF. The effect of electrospinning parameters such as polymer concentration and applied voltage on the AFD and morphology of the membranes was evaluated. It is found that both polymer concentration and applied voltage have great influence on both AFD and morphology of the fibrous membranes. It is observed that AFD increases with solution concentration and applied voltage. A fibrous membrane with uniform morphology and AFD of 350 nm was prepared under the optimized condition of 16 wt.% solution in DMF at 20 kV. The GPEs were prepared by activating the membrane with different liquid electrolytes. All the GPEs exhibited high ionic conductivity in the range of ~10^{-3} S cm^{-1} at 25 °C. The GPEs have good electrochemical stability >4.7 V versus Li/Li^+, and have a stable R_f value with lithium metal. Prototyped coin cells using GPEs based on electrospun PAN with 1 M $LiPF_6$ in EC/DMC or PC were evaluated with $LiFePO_4$ cathode for charge–discharge capacity and cycle performance. The resulting good discharge capacity and cycle performance indicate that GPEs based on electrospun PAN membranes are suitable for application in safe, reliable and long lasting lithium batteries.

Acknowledgement

This research was supported by Basic Science Research Program through the National Research Foundation (NRF) funded by the Ministry of Education, Science and Technology (KRF-2008-313-D00299).

References

[1] P. Raghavan, J.W. Choi, J.H. Ahn, G. Cheruvally, G.S. Chauhan, H.J. Ahn, A. Nah, J. Power Sources 184 (2008) 437.
[2] P. Raghavan, X. Zhao, J.K. Kim, J. Manuel, G.S. Chauhan, J.H. Ahn, C. Nah, Electrochim. Acta 54 (2008) 228.
[3] C.Y. Chiang, M.J. Reddy, P.P. Chu, Solid State Ionics 175 (2004) 631.
[4] Y.J. Wang, D. Kim, Electrochim. Acta 52 (2007) 3181.
[5] V. Gentili, S. Panero, P. Reale, B. Scrosati, J. Power Sources 170 (2007) 185.
[6] P. Raghavan, X. Zhao, J. Manuel, G.S. Chauhan, J.H. Ahn, H.S. Ryu, H.J. Ahn, K.W. Kim, C. Nah, Electrochim. Acta 55 (2010) 1347.
[7] X. Li, G. Cheruvally, J.K. Kim, J.W. Choi, J.H. Ahn, K.W. Kim, H.J. Ahn, J. Power Sources 167 (2007) 491.
[8] G. Cheruvally, J.K. Kim, J.W. Choi, J.H. Ahn, Y.J. Shin, J. Manuel, P. Raghavan, K.W. Kim, H.J. Ahn, D.S. Choi, C.E. Song, J. Power Sources 172 (2007) 863.
[9] J.K. Kim, G. Cheruvally, X. Li, J.H. Ahn, K.W. Kim, H.J. Ahn, J. Power Sources 178 (2008) 815.
[10] N.T.K. Sundaram, A. Subramania, Electrochim. Acta 52 (2007) 4987.
[11] G. Jiang, S. Maeda, H. Yang, Y. Saito, S. Tanase, T. Sakai, J. Power Sources 141 (2005) 143.
[12] A.I. Gopalan, P. Santhosh, K.M. Manesh, J.H. Nho, S.H. Kim, C.G. Hwang, K.P. Lee, J. Membr. Sci. 325 (2008) 683.
[13] Y.H. Liao, D.Y. Zhou, M.M. Rao, W.S. Li, Z.P. Cai, Y. Liand, C.L. Tan, J. Power Sources 189 (2009) 139.
[14] J.W. Choi, G. Cheruvally, Y.H. Kim, J.K. Kim, J. Manuel, P. Raghavan, J.H. Ahn, K.W. Kim, H.J. Ahn, D.S. Choi, C.E. Song, Solid State Ionics 178 (2007) 1235.
[15] A.D. Pasquier, F. Disma, T. Bowmer, A.S. Gozdz, G. Amatucci, M. Tarascon, J. Electrochem. Soc. 145 (1988) 472.
[16] Elf-Atochem's technical brochure, Kynar and Kynar Flex PVdF.
[17] F. Boudin, X. Andrieu, C. Jehoulet, I.I. Olsen, J. Power Sources 81–82 (1999) 804.
[18] S. Abbrent, J. Pletstil, D. Hlavata, J. Lindgren, J. Tegenfeldt, A. Wendsjo, Polymer 42 (2001) 1407.
[19] B. Huang, Z. Wang, L. Chen, R. Xue, F. Wang, Solid State Ionics 91 (1996) 279.
[20] H. Tsutsumi, A. Matsuo, K. Takase, S. Doi, A. Hisanaga, K. Onimura, T. Oishi, J. Power Sources 90 (2000) 33.
[21] K.M. Abraham, M. Alamgir, J. Electrochem. Soc. 137 (1990) 1657.
[22] H.S. Min, J.M. Ko, D.W. Kim, J. Power Sources 119–121 (2003) 469.
[23] G. Wu, H.Y. Yang, H.Z. Chen, F. Yuan, L.G. Yang, M. Wang, R.J. Fu, Mater. Chem. Phys. 104 (2007) 284.
[24] J.K. Kim, J.W. Choi, G. Chereuvally, J.U. Kim, J.H. Ahn, K.W. Kim, H.J. Ahn, Mater. Lett. 61 (2007) 3822.
[25] S.A. Theron, E. Zussmana, A.L. Yarin, Polymer 45 (2004) 2017.
[26] Z.M. Huang, Y.Z. Zhang, M. Kotaki, S. Ramakrishna, Compos. Sci. Technol. 63 (2003) 2223.
[27] S.W. Choi, S.M. Jo, W.S. Lee, Y.R. Kim, Adv. Mater. 15 (2003) 2027.
[28] J.Y. Kim, Y. Lee, D.Y. Lim, Electrochim. Acta 54 (2009) 3714.
[29] H.P. Wang, H. Huang, S.L. Wunder, J. Electrochem. Soc. 147 (2000) 2853.
[30] Y.M. Lee, J.W. Kim, N.S. Choi, J.A. Lee, W.H. Seol, J.K. Park, J. Power Sources 139 (2005) 235.
[31] J. Saunier, F. Alloin, J.Y. Sanchez, G. Caillon, J. Power Sources 119–121 (2003) 454.
[32] J.R. Kim, S.W. Choi, S.M. Jo, W.S. Lee, B.C. Kim, J. Electrochem. Soc. 152 (2005) A295.
[33] S.W. Choi, J.R. Kim, S.M. Jo, W.S. Lee, Y.R. Kim, J. Electrochem. Soc. 152 (2005) A989.
[34] J.R. Kim, S.W. Choi, S.M. Jo, W.S. Lee, B.C. Kim, Electrochim. Acta 50 (2004) 69.